第 30 卷第 12 期 无 机 化 学 学 报 Vol.30 No.12
2014 年 12 月 CHINESE JOURNAL OF INORGANIC CHEMISTRY 2863-2871

聚合羟基铁改性蒙脱石的制备、表征及吸附 Se(Ⅵ)的特性

杨小洪 魏世勇* 方 敦 但悠梦
(生物资源保护与利用湖北省重点实验室,湖北民族学院化学与环境工程学院,恩施 445000)

摘要: 采用共沉淀法制备了 3 种聚合羟基铁改性蒙脱石(Mt-Fe_x, x=1, 2, 3),对比研究了纯蒙脱石(Mt)和 Mt-Fe_x(x=1, 2, 3)的表面性质及吸附 Se(Ⅵ)的特性。结果表明,Mt 样品的 $d_{(001)}$ 层间距为 1.296 nm,在 Mt-Fe_x 中升高至 1.430 nm 以上;与 Mt 样品比较,Mt-Fe_x 的孔体积、表面积、表面分形度均随含铁量的增加而升高,其中微孔体积和微孔表面积的变化尤为明显;Mt 样品的等电点(IEP)低于 3,而 Mt-Fe_3 的 IEP 升高至 6.8;初始 pH=5.0 时,Mt 和 Mt-Fe_x(x=1, 2, 3)的表面 ζ 电位分别为−33.5, −11.7, 9.9 和 33.2 mV。单吸附位 Langmuir 模型能够很好地拟合 Mt 样品对 Se(Ⅵ)的等温吸附数据(R^2=0.993),4 种样品吸附数据的单吸附位 Langmuir 拟合判断系数(R^2)随样品含铁量的增加而降低;3 种 Mt-Fe_x 样品的吸附数据更适合用双吸附位 Langmuir 模型拟合(R^2=0.993~0.997);Freundlich 模型对 4 种样品的吸附数据拟合度较低(R^2=0.849~0.970),其判断系数(R^2)随样品含铁量的增加而升高。初始 pH=5.0 时,Mt 和 Mt-Fe_x(x=1, 2, 3)对 Se(Ⅵ)的吸附容量分别为 4.23, 7.83, 10.38 和 14.34 mg·g^{-1}。可见,聚合羟基铁含量较高的 Mt-Fe_x 样品对土−水体系中 Se(Ⅵ)的固定能力明显高于 Mt。

关键词: 蒙脱石; 聚合羟基铁改性蒙脱石; 表面性质; 吸附; 硒(Ⅵ)
中图分类号: O614.81; S153.6; P578.4 **文献标识码**: A **文章编号**: 1001-4861(2014)12-2863-09
DOI: 10.11862/CJIC.2014.385

Hydroxyiron Polymers-Modified Montmorillonite: Preparation, Characterization and Adsorption Characteristics for Selenate

YANG Xiao-Hong WEI Shi-Yong* FANG Dun DAN You-Meng
(*Key Laboratory of Biologic Resources Protection and Utilization of Hubei Province. Department of Chemistry and Environmental Engineering, Hubei University for Nationalities, Enshi, Hubei* 445000, *China*)

Abstract: Hydroxyiron polymers-modified montmorillonite (Mt-Fe_x, x=1, 2, 3) was prepared by a coprecipitation procedure. The surface properties and selenate (Se(Ⅵ)) adsorption of Mt-Fe_x were investigated and compared with those of pure montmorillonite (Mt). Results show that the $d_{(001)}$ spacing of Mt-Fe_x montmorillonite increases to more than 1.430 nm from 1.296 nm of the Mt. Compared to Mt, the pore volume, surface area and surface fractal dimension of Mt-Fe_x increase with increasing the Fe content. The increased quantities of the micropore volume and micropore surface area are very significantly. The isoelectric point (IEP) varies from the value of < 3 of the Mt to 6.8 of the Mt-Fe_3, and the surface ζ potential at pH value of 5.0 is −33.5, −11.7, 9.9, and 33.2 mV for Mt, Mt-Fe_1, Mt-Fe_2, and Mt-Fe_3, respectively. The Se(Ⅵ) adsorption data of Mt can be well fitted by one-site Langmuir model (R^2=0.993) and the R^2 of the four samples shows the order of Mt>Mt-Fe_1>Mt-Fe_2>Mt-Fe_3. As for Mt-Fe_x, two-site Langmuir model fits the adsorption data better than the one-site model. The coefficients of determination (R^2) obtained from Freundlich model of the samples are relatively low (R^2=0.849~0.970) and increase slightly with increasing the Fe content in Mt-Fe_x. This indicates that the surface of Mt-Fe_x possesses different types of reactive sites for Se(Ⅵ) adsorption. At pH=5.0, the adsorption capacities (q_{max}) of Mt, Mt-Fe_1, Mt-Fe_2, and Mt-Fe_3 are 4.23, 7.83, 10.38, and 14.34 mg·g^{-1},

收稿日期:2014-07-22。收修改稿日期:2014-09-11。
国家自然科学基金(No.41261060)和生物资源保护与利用湖北省重点实验室开放基金 (No.PKLHB1315)资助项目。
*通讯联系人。E-mail:xiangju12345@126.com

respectively. Mt-Fe_x with a high content of hydroxyiron polymers has a high adsorption capacity for the Se(Ⅵ) in soil and sediment solutions.

Key words: montmorillonite; hydroxyiron polymers-modified montmorillonite; surface properties; adsorption; selenate

0 Introduction

Selenium (Se) is an essential micronutrient for animals and humans [1-2]. There is no evidence that plants require Se for growth and completion of their life cycles, but the main source of dietary Se for humans and animals is plant material. Therefore, the Se levels in plants are also important to human health. In fact, there is a very narrow range between deficient and toxic levels of Se in mammals, and thus the toxicity and deficiency of Se occur frequently in the world[1,3-4]. Although the uptake and accumulation of Se by plants is largely dependent on the Se content in the soil, other factors, such as the constituents, pH value and redox conditions of soils that affect the transformation, adsorption, precipitation and bioavailability of Se compounds, are also involved[2,5-6]. Therefore, understanding interactions between soil constituents (e.g. Fe/Al (hydro-)oxides, organic matter, phyllosilicates, carbonates) and Se are vital to control the uptake of Se by plants from soils.

Iron oxides and hydroxyl polymers are ubiquitous in natural environments, and most of them possess a high surface area and a large amount of reactive surface hydroxyl sites (≡Fe-OH) [7-9]. Therefore, they have important effect on the migration and transformation of nutrients and pollutants in soils and sediments [10-12]. Phyllosilicates are an important solid component in soils and sediments and exert significant influences on their structures [5,10]. Although the adsorption capacity for anions onto phyllosilicates is low when compared to iron hydroxyl polymers and oxides, phyllosilicates are widely distributed in natural soils and thus play a certain role in the retention of nutrients and pollutants [10,12]. Montmorillonite, a well-defined 2:1-type phyllosilicate, is very common in soils. The main surface sites of montmorillonite are aluminol groups (≡Al-OH) situated at the edges and the hydroxyl-terminated planes [13-14]. In addition, the high permanent negative charges on the basal surfaces of montmorillonite may exert an important effect on the surface adsorption properties of colloid particles[14-15].

In soils iron oxides and hydroxyl polymers often tend to coat on the surfaces and/or enter into the interlayer spaces of phyllosilicates to form Fe-modified phyllosilicates [7,10]. The modification is very important to the physical and chemical properties of the clays in natural environments [10,14]. In suspension systems containing Fe hydroxyl ions and phyllosilicates, the interlayer spaces of 2:1-type phyllosilicates can be expanded to a certain extent because of ion exchange[13,16]. The porous structure, surface area and cation exchange capacity (CEC) of Fe-modified phyllosilicates are obviously different from the single phase phyllosilicates[10,13,16]. The point of zero charge (PZC) and the isoelectric point (IEP) of Fe-modified phyllosilicates increase compared to the single phase phyllosilicates, and the magnitude of the effect depends on the ratio of iron oxides to phyllosilicates as pointed by Tombácz et al[8] and Hou et al[17]. The modification of iron (hydro-)oxides on the surfaces of phyllosilicates decreases the negative charge density on phyllosilicates and the ζ potential of the clay colloidal particles moves to the positive value side[17-18].

The modification of iron hydroxyl polymers and oxides on phyllosilicates may exert an important influence on the adsorption properties for environment substances (e.g. heavy metal ions, inorganic anions, organic pollutants) onto mineral surface[10,13,16-19]. As for Se(Ⅵ), the adsorption properties on single phase iron oxides and montmorillonite have been extensively studied[6,9,13-15]. However, to the best of our knowledge, the adsorption behavior of Se(Ⅵ) onto hydroxyiron

polymers-modified montmorillonite (Mt-Fe_x) is not well documented. In this study several Mt-Fe_x samples with different contents of hydroxyiron polymers were prepared, and the adsorption properties for Se(Ⅵ) onto Mt-Fe_x were investigated and compared with those of pure montmorillonite (Mt). The obtained results may be helpful to understand the geochemical cycle of environmental Se(Ⅵ) and control the activity of Se(Ⅵ) in soils and sediments.

1 Experimental

1.1 Sample preparation

Raw montmorillonite was purchased from Zhejiang Sanding Technology Co., Ltd. (Shaoxing, China) and pretreated according to the following procedure: about 20 mL 30% H_2O_2 was added to 20 g raw montmorillonite in a 2 L glass flask under manual stirring to remove organic matter. Then the mineral particles were fractionated by the conventional sedimentation method. The particles (<2 μm fraction) in the suspension were treated with NaCl solution, centrifuged and washed with deionized water until free from chloride anions as tested by 0.1 mol·L^{-1} $AgNO_3$ solution, and then washed one time with 95% ethanol. The Na-saturated montmorillonite (Mt) was dialyzed against distilled water, freeze-dried, ground to pass a 60-mesh (250 μm) sieve, and stored in a desiccator.

For the preparation of hydroxyiron polymers-modified montmorillonite (Mt-Fe_x), at first three Mt suspensions were prepared as follows. 100 mL distilled water was added to 4.81 g Mt in a 1 L polyethylene flask, followed by vigorous stirring for 10 min and ultrasonic dispersion for 30 min. Then 11.1, 33.3 and 99.9 mL of 0.5 mol·L^{-1} $FeCl_3$ solution was poured into the Mt suspensions under vigorous magnetic stirring respectively. These amounts of Mt and $FeCl_3$ were selected in order to reach a theoretical mass ratio (1:9, 1:3, and 1:1) of ferrihydrite with the chemical composition $Fe_5HO_8 \cdot 4H_2O$ to Mt. The suspension was adjusted to pH=8.0 with a 6 mol·L^{-1} NaOH solution. After a reaction time of 240 min the stirring was stopped. The polyethylene flask was sealed and aged at rest for 5 d at room temperature. The prepared precipitate was dialyzed, dried, ground and stored in the same way as the Mt. The three products were denoted as Mt-Fe_1, Mt-Fe_2, and Mt-Fe_3 according to the Fe content from low to high, respectively.

1.2 Sample analysis

The content of Fe in Mt-Fe_x was determined as follows. 20 mg sample was dissolved in a 5 mL of 6 mol·L^{-1} HCl solution, oscillated for 8 h, and then centrifuged. The concentration of Fe in the supernatant was measured by a Varian Vista-MPX ICP-OES (ICP). Powder X-ray diffraction (XRD) patterns were recorded on a Bruker D8 ADVANCE X-ray diffractometer equipped with a Lynx-Eye detector using Cu $K\alpha 1$ radiation (λ =0.154 06 nm). The diffractometer was operated at 40 kV tube voltage and 40 mA tube current with a scanning rate of 2°·min^{-1} at a step size of 0.02°. The N_2 adsorption-desorption experiments were performed at 77 K with Quanta Chrome Autosorb-1S apparatus. 0.20 g powder sample was degassed for 16 h at 80 ℃ prior to the measurement. The total pore volume was calculated from the maximum adsorption capacity at relative pressure close to the saturation pressure. The specific surface area and surface fractal dimension of the samples were calculated from the N_2 adsorption isotherms according to Brunauer-Emmett-Teller (BET) and Frenkel-Halsey-Hill (FHH) model, respectively. The micropore volume, micropore surface area, and external surface area were calculated from the N_2 adsorption isotherms according to *t*-plot micropore analysis. The ζ potential analyzer (ZetaSizer, Malvern Instruments Corporation) was used to determine the isoelectric point (IEP) and ζ potential by the ζ potential function of pH value in 0.02 mol·L^{-1} NaCl.

1.3 Adsorption experiments

For preparation the 10 g·L^{-1} stock suspension of adsorbents, 5 g sample and 300 mL distilled water were added into a 500 mL polyethylene flask, followed by ultrasonic dispersion for 30 min, and then the volume of the suspension was adjusted to 500 mL with distilled water. A 400 mg·L^{-1} Se(Ⅵ) stock solution was prepared by dissolving Na_2SeO_4 in distilled water.

Batch adsorption experiments were conducted with a 2 $g \cdot L^{-1}$ adsorbent concentration, 0.02 $mol \cdot L^{-1}$ NaCl background electrolyte, a set of initial Se(Ⅵ) concentrations (1~200 $mg \cdot L^{-1}$) and a temperature of 25 ℃. A 10 mL adsorbent suspension and 0~10 mL of Se(Ⅵ) stock solution were taken into a 50 mL stoppered conical flask, followed by adding 4 mL of 0.1 $mol \cdot L^{-1}$ NaCl to maintain ionic strength. The pH value of the suspension was adjusted to 5.0, and then the volume was adjusted to 20 mL with distilled water. The suspension was mechanically agitated at a speed of 300 $r \cdot min^{-1}$ for 24 h, and then filtered through a 0.45-μm membrane filter. The Se(Ⅵ) concentration in the filtrate was analyzed by inductively coupled plasma atomic emission spectrometry (ICP-AES). All experiments were performed in triplicate, and the average values were reported in present study. The adsorption capacity for Se(Ⅵ) by the adsorbents was calculated from the following equation:

$$q_e = (c_i - c_e)/c_A \quad (1)$$

where q_e ($mg \cdot g^{-1}$) is the adsorption capacity, c_i and c_e ($mg \cdot L^{-1}$) is the initial and residual concentration of Se(Ⅵ) respectively, and c_A ($g \cdot L^{-1}$) is the adsorbent concentration.

2 Results and discussion

2.1 Characterization of the samples

The content of Fe in Mt-Fe_x is 5.1%, 11.7% and 23.4% (*w*/*w*), respectively. This indicates that the content of Fe in Mt-Fe_x increases with increasing the initial ratio of $FeCl_3$ to Mt. The XRD patterns of the samples are shown in Fig.1. The peaks of Mt match well with the PDF cards of montmorillonite (PDF No. 12-0204), indicating that Mt possesses a good crystallinity and a high purity. In the XRD patterns of Mt-Fe_x (x=1, 2, 3), all the diffraction peaks may be assigned to montmorillonite and no XRD peak of iron oxides is detected. This indicates that no crystalline iron oxide is formed and amorphous hydroxyiron polymers are present in Mt-Fe_x. The $d_{(001)}$ spacing of montmorillonite in Mt-Fe_x increases to the value of > 1.400 nm from 1.296 nm of the Mt. This implies that some of the interlayered Na^+ ions in Mt are replaced by hydroxyiron ions during the formation process of Mt-Fe_x[10,13]. However, in Mt-Fe_x(x=1, 2, 3) the increased montmorillonite $d_{(001)}$ spacing and the contents of Fe do not show a positive relation. Compared to Mt, the diffraction peaks of montmorillonite in Mt-Fe_x show much lower intensity and broader width. This can be attributed to the factor that the hydroxyiron polymers in Mt-Fe_x coat some of montmorillonite surfaces and reduce the preferred orientation of montmorillonite[10,19].

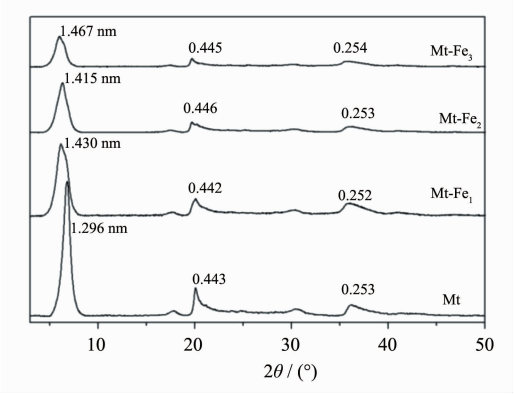

Fig.1 XRD patterns of the samples

Fig.2 presents N_2-physi-sorption isotherms of the samples. Generally, the four adsorption isotherms are similar and the monolayer adsorption capacity of N_2 by the samples increases in the order of Mt<Mt-Fe_1< Mt-Fe_2<Mt-Fe_3. According to IUPAC-classification[20], the isotherms of the samples belong to the type IV, which is characteristic of a type H2 hysteresis loop caused by capillary condensation. This indicates that the samples possess a number of micropores and mesopores. At the low relative pressure (p/p_0<0.4) the adsorption is due to micropores (<2 nm) and at higher relative pressure

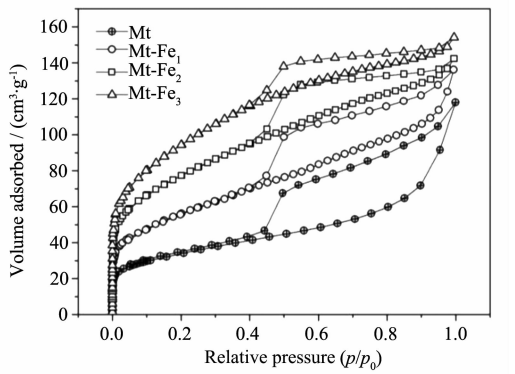

Fig.2 Nitrogen adsorption/adsorption isotherms of the samples

(p/p_0 >0.4) a wide hysteresis loop indicates a high distribution of mesopores (2 ~50 nm)[11,20-22]. The N_2 volumes adsorbed significantly increase at low relative pressure and the hysteresis loop becomes narrow at higher relative pressure as evidenced by comparing the isotherms of the different samples, from Mt to Mt-Fe_3. This indicates that the volume ratio of micropores to mesopores for the samples increases with increasing the content of hydroxyiron polymers. This can be attributed to the factors that: (1) most of the total pore volume of amorphous hydroxyiron polymers is due to micropores[11] and most of the total pore volume of montmorillonite due to mesopores[21-22]; and (2) the expansion of the $d_{(001)}$ spacing of montmorillonite in Mt-Fe_x increases the micropore volume of Mt-Fe_x.

Table 1　Surface structural properties of the samples

Sample	Total pore volume / ($cm^3 \cdot kg^{-1}$)	Micropore volume / ($cm^3 \cdot g^{-1}$)	BET surface area / ($m^2 \cdot g^{-1}$)	Micropore surface area / ($m^2 \cdot g^{-1}$)	External surface area / ($m^2 \cdot g^{-1}$)	Surface fractal dimension D
Mt	0.147	0.043	123	56	66	2.39
Mt-Fe_1	0.167	0.071	161	88	70	2.51
Mt-Fe_2	0.179	0.086	186	113	73	2.57
Mt-Fe_3	0.214	0.129	248	166	79	2.61

The pore volumes and surface areas of the samples are listed in Table 1. All these porous parameters increase in the order of Mt <Mt-Fe_1 <Mt-Fe_2 <Mt-Fe_3. This indicates that the porous structure of montmorillonite is improved due to the modification of hydroxyiron polymers. One may note that the increased quantities of micropore volumes and micropore areas are very significant and that of external surface areas are slight. This once again indicates that the hydroxyiron polymers in Mt-Fe_x are microporous. Surface fractal dimension of mineral sample is considered as an operative index of surface roughness. The D value of surface fractal dimension obtained by FHH method, which accounts for adsorbate surface tension effects, is between **2** and **3**. A low D value means a regular and smooth surface and a higher D value suggests a coarser surface[22-23]. The D values of the four samples imply that the surface roughness and pore structural heterogeneity of the samples increase with the increase in the Fe content.

Fig.3 shows the pH-ζ potential curves of the samples. The values of ζ potential of the four samples decrease with increasing the pH value of the colloid suspensions. This can be interpreted in terms of the mechanism of the variable charge generation. With increasing the pH value of the suspension, the deprotonation of the hydroxyl groups on sample surface results in the decrease in the surface charge and ζ potential of the samples. With increasing the Fe content the decrease in the ζ potential of the four samples becomes more significant when the pH value varies from **3** to **9**. This can be attributed to the fact that the charge on montmorillonite surface mainly is permanent and that on hydroxyiron polymers mainly is variable[8-9,15].

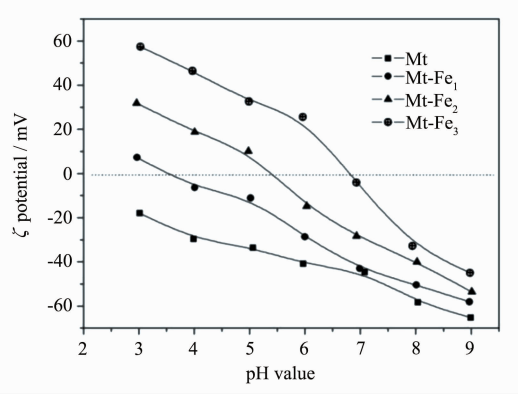

Fig.3　pH-ζ potential curves of the samples

In the pH-ζ potential curves the pH value at the ζ potential value of zero is regarded as isoelectric point (IEP). From Fig.3, the modification of hydroxyiron polymers on montmorillonite surface increases the IEP value of the samples from < 3 of Mt to 3.6 of Mt-Fe_1, 5.4 of Mt-Fe_2, and 6.8 of Mt-Fe_3, respectively. The overlapping of the diffusion layers

on hydroxyiron polymers and montmorillonite colloid particles decreases the effective negative surface charge density on montmorillonite and thus leads to an increase in the IEP of Mt-Fe$_x$. When the pH value of colloid suspension is lower than the IEP the zeta potential on the sample surface is positive, otherwise negative ζ potential occurs. At pH=5.0, the surface ζ potential value of Mt, Mt-Fe$_1$, Mt-Fe$_2$ and Mt-Fe$_3$ is −33.5, −11.7, 9.9 and 33.2 mV, respectively. Clearly, negative ζ potential occurs on the surfaces of Mt and Mt-Fe$_1$, and positive ζ potential on the surfaces of Mt-Fe$_2$ and Mt-Fe$_3$. These differences in the surface zeta potential may influence significantly the surface adsorption properties of the samples, which will be further discussed in the adsorption properties for Se(Ⅵ) by the four samples.

2.2 Se(Ⅵ) adsorption by the samples

The isotherm adsorption data for Se(Ⅵ) by the samples are shown in Fig.4, and they are fitted using the classical one-site Langmuir, two-site Langmuir and Frieundlich models (see Eqs.(**2**)~(**4**), respectively).

$$q_e = q_{max} b c_e/(1+bc_e) \quad (2)$$

$$q_e = q_1 b_1 c_e/(1+b_1 c_e) + q_2 b_2 c_e/(1+b_2 c_e) \quad (3)$$

$$q_e = k c_e^{1/n} \quad (4)$$

where q_e (mg·g^{-1}) is the amount for Se(Ⅵ) adsorbed and c_e (mg·L^{-1}) is the equilibrium concentration of Se(Ⅵ) in bulk solution, q_{max} (mg·g^{-1}) and b (L·mg^{-1}) are the adsorption capacity and energy constant (affinity coefficient) for one-site Langmuir model, respectively[24-25]. q_1 and q_2 (mg·g^{-1}) are the adsorption capacities for the high- and low-energy sites on the surface respectively, and the total adsorption capacity (q_t, mg·g^{-1}) is quantified as q_1+q_2. b_1 and b_2 (L·mg^{-1}) are the corresponding affinity coefficients in the two-site Langmuir model[26-27]. k (mg$^{1-(1/n)}$·L$^{1/n}$·g^{-1}) and n (dimensionless) are the Freundlich constants related to the adsorption capacity and intensity, respectively[28-29].

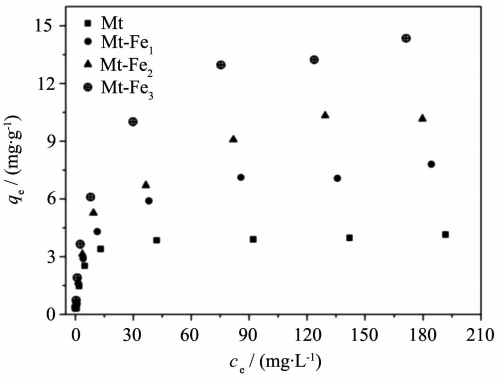

(adsorbent dose: 2 g·L^{-1}; temperature: 25 ℃; background electro lyte: 0.02 mol·L^{-1} NaCl; contact time: 24 h; pH=5.0)

Fig.4 Adsorption data for Se(Ⅵ) by the samples

The fitting results of the adsorption data to the adsorption models are summarized in Table 2. The apparent affinity constants (b) obtained from one-site Langmuir model decreases in the order of Mt>Mt-Fe$_1$> Mt-Fe$_2$ >Mt-Fe$_3$. According to literatures[7-9,13-15], the main functional group on hydroxyiron polymers for adsorption anion is hydroxyl Fe, and on montmorillonite is hydroxyl Al. Therefore, the results show that the adsorption affinity for Se(Ⅵ) of hydroxyl Al is higher than that of hydroxyl Fe. The Se(Ⅵ) adsorption capacities (q_{max}) of the samples follow the order of Mt-Fe$_3$>Mt-Fe$_2$>Mt-Fe$_1$>Mt, indicating that the modification of hydroxyiron polymers on montmorillonite enhances significantly the adsorption capacity for Se(Ⅵ) onto the samples. The coefficients of determination (R^2) are all higher than 0.960 and they decrease slightly from 0.993 of Mt to 0.963 of Mt-Fe$_3$. This indicates that one-site Langmuir model is very suitable to represent Se(Ⅵ) adsorption onto Mt surface.

The two-site Langmuir model considers that Se(Ⅵ) is adsorbed by different energy sites on the surface of the samples. As for Mt, the two affinity coefficients are equal (b_1/b_2=1.00) and the adsorption capacities are very similar (q_1/q_2=0.99). Moreover, the coefficient of determination for Mt obtained from one-site Langmuir model is equal to that from the two-site model (R^2=0.993). These results indicate that the two hypothetical adsorption sites in the two-site model should be degenerated to one site for pure Mt. The total adsorption capacities (q_t) of Mt-Fe$_x$ derived by two-site Langmuir model are larger than the corresponding q_{max} obtained by one-site model. As for every Mt-Fe$_x$, the affinity coefficients for high-energy sites (b_1) are much higher than those for low-energy sites (b_2). The ratios of b_1 to b_2 of Mt-Fe$_x$ show the

order of Mt-Fe_1>Mt-Fe_2≈Mt-Fe_3. For Mt-Fe_1, Mt-Fe_2 and Mt-Fe_3, the adsorption capacities ratio (q_1/q_2) decreases from 1.53 to 0.94, and to 0.65. It again indicates that: (1) the high-energy adsorption site for Se(Ⅵ) is the hydroxyl Al on montmorillonite and the low-energy site is the hydroxyl Fe on hydroxyiron polymers, and (2) in Mt-Fe_x the Se(Ⅵ) adsorption capacity of hydroxyiron polymers is much higher than that of montmorillonite. The q value is an apparent adsorption capacity under the experimental conditions and does not necessarily equal to the total amount of the corresponding sites. The determination coefficient (R^2) of Mt-Fe_x obtained from two-site Langmuir model (R^2=0.992~0.996) is higher than that from one-site model (R^2=0.989~0.963). This indicates that two-site Langmuir model fits the adsorption data of Mt-Fe_x better than the one-site model.

The Freundlich adsorption constants (k) of the samples increase in the sequence of Mt<Mt-Fe_1<Mt-Fe_2<Mt-Fe_3, which is in agreement with that of the Langmuir adsorption capacities. The Freundlich adsorption intensity parameters (n) of the samples reduce from 4.36 of Mt to 2.84 of Mt-Fe_3. The sequence of the n value for the four samples is in agreement with that of the Langmuir adsorption apparent affinity (b), indicating that the adsorption affinity for Se(Ⅵ) decreases with increasing the Fe content in the samples. The determination coefficient (R^2) of Mt obtained from Freundlich model is relatively low (R^2=0.849) and that of Mt-Fe_x increases slightly with increasing the Fe content.

Selanate adsorption properties of adsorbents are dependent on the surface properties of adsorbents[9,13-15]. All the adsorption capacities of Mt-Fe_x are higher than that of pure Mt (Fig.4 and Table 2). This can be understood by the following reasons. Firstly, the pore volumes, surface areas, and surface fractal dimension D of Mt-Fe_x are higher than those of Mt (Table 1). These differences in the surface properties may contribute to a greater amount of Se(Ⅵ) adsorption onto Mt-Fe_x than onto Mt[9,13,19]. Secondly, the Mt is provided with an extremely low IEP (<3.0) and a negative surface zeta potential at pH =5.0 (−33.5 mV). Compared to Mt, Mt-Fe_x (x=1, 2, 3) have higher IEP (3.6, 5.4, and 6.8, respectively) and surface ζ potential at pH=5.0 (−11.7, 9.9, and 33.2 mV, respectively). This indicates that the electrostatic repulsion between Se(Ⅵ) anions and the surface negative charge of the samples decreases and even turns gradually into an electrostatic attraction with increasing the Fe content in Mt-Fe_x. Thirdly, the bonding bridge is a common adsorption mechanism for anions onto binary and ternary systems[19,27,30]. In the colloid suspensions of Mt-Fe_x, Se(Ⅵ) anions may act as a bridge to bond the two interfaces of montmorillonite and hydroxyiron polymers. In addition, Se(Ⅵ) anions adsorption onto clay minerals has been shown to occur largely through ligand exchange at surface hydroxyl sites[9,14]. The reactive hydroxyl sites of hydroxyiron polymers are spread over its entire surface[8,19], while ≡Al-OH sites on phyllosilicates surface are located exclusively at the edges of its crystal structure[8,15]. This indicates that the density of reactive hydroxyl sites on the hydroxyiron polymers is greater in comparison with montmorillonite. Finally, the particle size of hydroxyiron polymers in Mt-Fe_x is very small, and probably a special nanoscale size-effect also contributes to a higher Se(Ⅵ) adsorption onto Mt-Fe_x[19]. Generally, the hydroxyiron polymers-modified montmorillonite, Mt-Fe_3-like, has a high adsorption

Table 2　Adsorption model parameters of Se(Ⅵ) onto the samples.

Sample	one-site Langmuir			two-site Langmuir				Freundlich		
	q_{max} / (mg·g^{-1})	b / (L·mg^{-1})	R^2	q_t / (mg·g^{-1})	q_1 / q_2	b_1 / b_2	R^2	k / (mg$^{1-(1/n)}$·L$^{1/n}$·g^{-1})	n	R^2
Mt	4.23	0.262	0.993	4.22	0.99	1.00	0.993	1.38	4.36	0.849
Fe-Mt_1	7.83	0.117	0.989	9.14	1.53	19.31	0.992	1.66	3.21	0.949
Fe-Mt_2	10.38	0.091	0.965	12.05	0.94	15.35	0.997	1.91	2.96	0.963
Fe-Mt_3	14.34	0.085	0.963	16.92	0.65	15.49	0.996	2.55	2.84	0.970

capacity for Se(Ⅵ) and is important to the retention of Se(Ⅵ) in soils and sediments.

As for Mt, the main reactive hydroxyl sites are ≡Al-OH groups located exclusively at the edges of the crystal structure [13-14], and the surface fractal dimension D value is relatively low (Table 1). This indicates that the Mt possesses a homogeneous surface with a finite number of identical sites for adsorption Se(Ⅵ). Therefore, the adsorption data for Se(Ⅵ) by the Mt can be well described using one-site Langmuir model, meaning that mono-layer mode is an important adsorption mechanism for Se(Ⅵ) onto Mt. For Mt-Fe$_x$, the main surface sites include the ≡Fe-OH groups that originate from hydroxyiron polymers and ≡Al-OH groups from montmorillonite. Therefore, two-site Langmuir model fits the data of Mt-Fe$_x$ much better than the one-site model. Although the Freundlich determination coefficients (R^2) of the four samples are relatively low, they increase from 0.849 of Mt to 0.970 of Mt-Fe$_3$. This can be attributed to the factors: (1) the D values of the samples increase with increasing the content of hydroxyiron polymers, and (2) as for Mt-Fe$_2$ and Mt-Fe$_3$, except for ≡Al-OH and ≡Fe-OH groups the surface positive charge is also an adsorption site for Se(Ⅵ). Mt-Fe$_x$ possesses a more heterogeneous surface with various adsorption sites when increasing the content of hydroxyiron polymers. Therefore, the R^2 from Freundlich model of the samples increases in the order of Mt<Mt-Fe$_1$<Mt-Fe$_2$<Mt-Fe$_3$, which means that multi-layer adsorption is also a mode of the Se(Ⅵ) retention onto Mt-Fe$_x$. These results lead to a better understanding of Se(Ⅵ) adsorption by hydroxyiron-clay associations, and also demonstrate that the modification of hydroxyiron polymers on clays in soils and sediments is important to the migration and bioavailability of environmental Se.

3 Conclusions

The surface properties of Mt are influenced significantly by the modification of hydroxyiron polymers, and the quantities of the effect show a positive correlation with the content of Fe in Mt-Fe$_x$ (x =1, 2, 3). Compared to Mt, the $d_{(001)}$ spacing of montmorillonite in Mt-Fe$_x$ is expanded; the porous structures of Mt-Fe$_x$ are greatly improved; and the IEP and the surface ζ potential at pH =5.0 increase to some extent. The Se(Ⅵ) adsorption data of the samples can be fitted by one-site Langmuir model and the determination coefficients (R^2) of the four samples show the order of Mt>Mt-Fe$_1$>Mt-Fe$_2$>Mt-Fe$_3$. As for Mt-Fe$_x$, two-site Langmuir model fits the adsorption data better than the one-site model. The determination coefficient (R^2) obtained from Freundlich model of Mt is relatively low and that of Mt-Fe$_x$ increases slightly with increasing the content of hydroxyiron polymers. The Langmuir adsorption capacities (q_{max} and q_1) and Freundlich adsorption capacity constants (k) for Se(Ⅵ) by Mt-Fe$_x$ are higher than those of Mt. Results in present study show that Mt-Fe$_x$ possesses a heterogeneous surface with different types of reactive sites and has a high adsorption capacity for Se(Ⅵ). Probably, monolayer and multilayer adsorption behaviors are simultaneously involved in the Se(Ⅵ) adsorption onto Mt-Fe$_x$.

References:

[1] Fernández-Martínez A, Charlet L. *Rev. Environ. Sci. Biotechnol.*, **2009**,**8**(1):81-110

[2] Van Dorst S H, Peterson P J. *J. Sci. Food Agric*., **1984**,**35**(6): 601-605

[3] Tan J A, Zhu W, Wang W, et al. *Sci. Total Environ*., **2002**, **284**(1):227-235

[4] Masscheleyn P H, Delaune R D, Patrick Jr W H. *J. Environ. Sci. Health A*, **1991**,**26**(4):555-573

[5] Neal R H, Sposito G, Holtzclaw K M, et al. *Soil Sci. Soc. Am. J.*, **1987**,**51**:1161-1169

[6] Peak D, Sparks D L. *Environ. Sci. Technol*., **2002**,**36**:1460 -1466

[7] Davey B G, Russell J D, Wilson M J. *Geoderma*, **1975**,**14**: 125-138

[8] Tombácz E, Libor Z, Illés E, et al. *Org. Geochem*., **2004**,**35**: 257-267

[9] Manceau A, Charlet L. *J. Colloid Interface Sci.*, **1994**,**168**:87-93

[10]Dimirkoua A, Ioannoub A, Doulaa M. *Adv.Colloid Interface*, **2002**,**97**:37-61

[11]Cornell R M, Schwertmann U. *The Iron Oxides*: *Structure*,

Properties, *Reactions*, *Occurences*, *Uses*. Weinheim: Wiley-VCH, **2003**:102-109

[12]Violante A, Pigna M. *Soil Sci. Soc. Am. J.*, **2002**,**66**:1788-1796

[13]Saha U K, Liu C, Kozak L M, et al. *Soil Sci. Soc. Am. J.*, **2004**,**68**:1197-1209

[14]Peak D, Saha U K, Huang P M. *Soil Sci. Soc. Am. J.*, **2006**, **70**:192-203

[15]Bar-Yosef B, Meek D. *Soil Sci.*, **1987**,**144**:11-19

[16]Yan L, Xu Y, Yu H, et al. *J. Hazard. Mater.*, **2010**,**179**:244-250

[17]Hou T, Xu R K, Zhao A Z. *Colloid. Surfaces A*, **2007**,**297**:91-94

[18]Lo S L, Chen T Y. *Chemosphere*, **1997**,**35**(5):919-930

[19]Wei S Y, Tan W F, Liu F, et al. *Geoderma*, **2014**,**213**:478-484

[20]Wei S Y, Xiang W J. *J. Food Agric. Environ.*, **2012**,**10**(1):923-929

[21]Yuana P, Fana M, Yanga D, et al. *J. Hazard. Mater.*, **2009**,**166**:821-829

[22]Wang C C, Juang L C, Lee C K, et al. *J. Colloid Interface Sci.*, **2004**,**280**:27-35

[23]Lee C K, Tsay C S. *J. Phys. Chem. B*, **1998**,**102**:4123-4130

[24]Langmuir I. *Soil Sci. Soc. Am. J.*, **1916**,**40**:1361-1368

[25]Wisawapipat W, Kheoruenromne I, Suddhiprakarn A, et al. *Geoderma*, **2009**,**153**:408-415

[26]Sposito G. *Soil Sci. Soc. Am. J.*, **1982**,**46**:1147-1152

[27]Wu X M, Zhang Y, Dou X M, et al. *Chemosphere*, **2007**,**69**:1758-1764

[28]Freundlich H M F. *J. Phys. Chem. B*, **1906**,**57**:385-470

[29]Yan L, Xu Y, Yu H, et al. *J. Hazard. Mater.*, **2010**,**179**:244-250

[30]Chan Y T, Kuan W H, Chen T Y, et al. *Water Res.*, **2009**, **43**:4412-4420